MATERIALS CHARACTERIZATION AT UTAH STATE UNIVERSITY: FACILITIES AND KNOWLEDGEBASE OF ELECTRONIC PROPERTIES OF MATERIALS APPLICABLE TO SPACECRAFT CHARGING

J.R. Dennison
Physics Department, Utah State University
Logan, UT, USA 84322-4415
Phone: 435.797.2936
Fax: 436.797.2492
E-mail: JR.Dennison@usu.edu

C.D. Thomson
J. Kite
V. Zavyalov
Jodie Corbridge
Physics Department, Utah State University

Abstract

In an effort to improve the reliability and versatility of spacecraft charging models designed to assist spacecraft designers in accommodating and mitigating the harmful effects of charging on spacecraft, the NASA Space Environments and Effects (SEE) Program has funded development of facilities at Utah State University for the measurement of the electronic properties of both conducting and insulating spacecraft materials. We present here an overview of our instrumentation and capabilities, which are particularly well suited to study electron emission as related to spacecraft charging. These measurements include electron-induced secondary and backscattered yields, spectra, and angular resolved measurements as a function of incident energy, species and angle, plus investigations of ion-induced electron yields, photoelectron yields, sample charging and dielectric breakdown. Extensive surface science characterization capabilities are also available to fully characterize the samples *in situ*. Our measurements for a wide array of conducting and insulating spacecraft materials have been incorporated into the *SEE Charge Collector Knowledgebase* as a *Database of Electronic Properties of Materials Applicable to Spacecraft Charging*. This *Database* provides an extensive compilation of electronic properties, together with parameterization of these properties in a format that can be easily used with existing spacecraft charging engineering tools and with next generation plasma, charging, and radiation models. Tabulated properties in the *Database* include: electron-induced secondary electron yield, backscattered yield and emitted electron spectra; He, Ar and Xe ion-induced electron yields and emitted electron spectra; photoyield and solar emittance spectra; and materials characterization including reflectivity, dielectric constant, resistivity, arcing, optical microscopy images, scanning electron micrographs, scanning tunneling microscopy images, and Auger electron spectra. Further details of the instrumentation used for insulator measurements and representative measurements of insulating spacecraft materials are provided in other Spacecraft Charging Conference presentations. The NASA Space Environments and Effects Program, the Air Force Office of Scientific Research, the Boeing Corporation, NASA Graduate Research Fellowships, and the NASA Rocky Mountain Space Grant Consortium have provided support.

Introduction

Up to one third of all spacecraft system anomalies and component failures are known to result from spacecraft charging [*1*]. Charging to high potentials can also lead to satellite material alterations and degraded instrumentation performance [*1-3*], as well as potential safety hazards for astronauts [4]. The extent and configurations of spacecraft charge buildup depends on spacecraft position and orientation, local environment parameters such as incident charged particle and photon flux, and material properties such as electrical properties (*e.g.,* resistivity and capacitance) and electron emission rates.

In an effort to improve the reliability and versatility of spacecraft charging models designed to assist spacecraft designers in accommodating and mitigating the harmful effects of charging on spacecraft, NASA, ESA and other agencies have developed an extensive set of engineering tools to predict the extent of charging in various spacecraft environments (e.g., NASCAP/LEO /GEO, POLAR, SEE Charging Handbook, NASCAP2K, SPARCS) [5-9]. The NASA Space Environments and Effects (SEE) Program is currently funding further extensions of the NASCAP2K charging code [6]. These codes model the spacecraft geometry orbit and orientation; plasma environment and particle flux; relevant materials properties; and charge absorption, distribution, transport and emission.

The original NASCAP databases lack relevant electronic properties of most spacecraft materials commonly in use today (only nine basic materials were incorporated in the original NASCAP database, [5]) so that many new spacecraft bulk materials and coatings need to be characterized. In addition, future charging codes will require better descriptions of materials properties plus the capability to model more complex materials and the effects of the evolution of materials properties due to contamination and other environmental effects [10-12]. Further, the codes will need to model more complex interactions between the emitted particles, charged spacecraft, ambient plasma environment and high-energy particle fluxes; this requires more sophisticated knowledge of the energy and angular trajectories of emitted and returning charged particles [13].

To enhance the effectiveness of these models, NASA SEE also sponsors the development of facilities and materials testing at Utah State University (USU) for measurement of the electronic properties of both conducting and insulating spacecraft materials [14,15]. The USU Materials Physics Group performs state-of-the-art ground-based testing of electronic properties of materials, particularly of electron emission and conductivity. Through the development of controlled ground-based experiments in vacuum chambers, essential electron yield parameters can be measured to update charging databases. In the laboratory, we use our knowledge of satellite-plasma environment interactions to design experiments that will provide us with an understanding of fundamental particle and material interactions that can occur in space. The objectives of the USU research are (i) to provide more accurate measurements together with sufficient materials characterization, (ii) to significantly extend the database to include a wider range of materials that are more representative of the myriad materials used in spacecraft design, (iii) to incorporate results of materials testing in parameterized form into electronic databases that are readily used by the charging codes, (iv) to explore extensions to the current modeling of these materials properties, and (v) to investigate additional charging topics such as the effects of contamination [9,11,16] or angular distribution of emitted electrons [13,16].

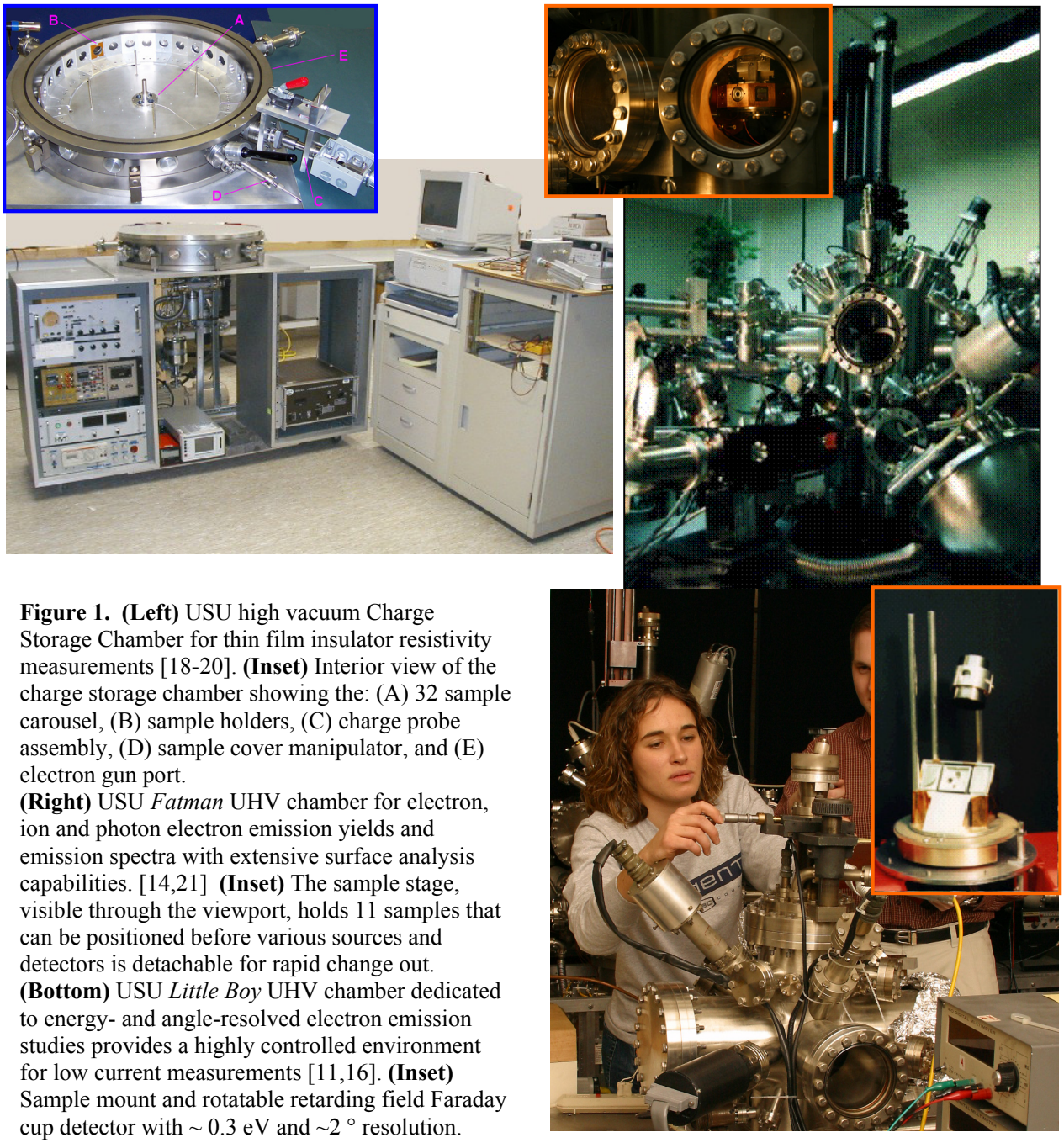

Figure 1. (Left) USU high vacuum Charge Storage Chamber for thin film insulator resistivity measurements [18-20]. **(Inset)** Interior view of the charge storage chamber showing the: (A) 32 sample carousel, (B) sample holders, (C) charge probe assembly, (D) sample cover manipulator, and (E) electron gun port.
(Right) USU *Fatman* UHV chamber for electron, ion and photon electron emission yields and emission spectra with extensive surface analysis capabilities. [14,21] **(Inset)** The sample stage, visible through the viewport, holds 11 samples that can be positioned before various sources and detectors is detachable for rapid change out.
(Bottom) USU *Little Boy* UHV chamber dedicated to energy- and angle-resolved electron emission studies provides a highly controlled environment for low current measurements [11,16]. **(Inset)** Sample mount and rotatable retarding field Faraday cup detector with ~ 0.3 eV and ~2 ° resolution.

In this paper, we begin with a description of the USU facilities and instrumentation [15,17,18], followed by a more detailed description of the specific required measurements and experimental methods used along with parameterization of materials properties for use with existing charging codes [13,14,19,21-23]. Representative measurements and analysis for a wide variety of materials are presented to illustrate these capabilities [22-24]. We also describe incorporation of our results into electronic databases [24]. A complete list of the materials already studied and those currently being tested are presented, as well as a justification of their selection for study [24]. We end with a review of recommendations for extensions to the parameterization of materials properties that should be incorporated into future charging models and a summary of additional related studies being performed at USU.

USU Facilities

This section provides an overview of our instrumentation and capabilities, which are particularly well suited to study electron emission and associated properties of both insulators and conductors, as related to spacecraft charging. These measurements include electron-induced SE and BSE yields, emission spectra, and angular resolved measurements as a function of incident energy, species and angle, plus investigations of ion-induced electron yields and emission spectra, photoelectron yields, conductivity, charge storage decay, internal sample charging, and dielectric breakdown. USU maintains three vacuum chambers with extensive space environment simulation capabilities (see Fig. 1). Other surface science and test capabilities are also available to fully characterize the samples.

Fatman surface analysis chamber

The primary instrument of the USU facility is a versatile ultra-high vacuum (UHV) chamber with surface analysis and sample characterization capabilities (see Fig. 1) [14-21]. This chamber can simulate diverse space environments including controllable vacuum ($<10^{-10}$ to 10^{-3} Torr) and ambient neutral gases conditions, temperature (<100 to >1500 K), electron fluxes, ion fluxes, and solar irradiation. The sample stage, visible through the viewport in Fig. 1, holds 11 samples that can be positioned before various sources and detectors and is detachable for rapid change out.

Electron sources include a low-energy gun (50 eV to 5 keV) and a high-energy gun (4 keV to 30 keV). Both guns provided monoenergetic electron beams ($\Delta E/E<2\cdot10^{-4}$) with beam currents ranging from 0.1 nA to 10 μA, beam spot diameters ranging from ~50 μm to 2 mm (depending on beam energy), and pulsing capabilities from 1 μs to continuous emission. There are three ion guns with <0.1 to 5 keV mono-energetic sources for inert and reactive gases, one with rastering and pulsed deflection capabilities. The NIR-VIS-UV solar irradiance spectrum is simulated using a pair of monochromated lamp sources: (i) a Tungsten/halogen lamp system with a *Suprasil* envelope produces focused (~0.5 cm diameter) radiation from 0.4 eV to 7.2 eV (200 nm to 2000 nm) and (ii) a Deuterium RF powered continuum source with a MgF_2 window produces focused (~0.5 cm diameter) radiation from 3.1 eV to 11.1 eV (150 nm to 400 nm). Radiation from these sources passes through a nitrogen-purged monochromator. A UV Si photodiode was calibrated against a pyroelectric detector, as a UHV-compatible secondary intensity standard. Additional light sources include a helium resonance lamp (21.2 and 40.8 eV), broadband Hg discharge and W-filament sources; and a variety of quasi-monochromatic NIR/VIS/UVA LED sources.

The primary detector for emission studies is a custom hemispherical grid retarding field analyzer fully enclosing the sample, and particularly well suited and calibrated for absolute yield measurements [14,21,23]. The hemispherical grid detection system has been carefully calibrated (both through calculation and measurement) to account for detector losses, allowing yield accuracies of better than 5%. The suppression grid is used to discriminate between BSE's (energies >50 eV) and SE's (energies <50 eV). By ramping the grid bias, energy spectra of the emitted electrons can also be measured using this detector. For conducting samples, electron guns are operated in continuous emission mode, and dc-currents are measured with standard ammeters sensitive to several tens of picoamperes. For pulsed measurements on insulators, the electron guns deliver 5 μs, 20-60 nA incident pulses. Custom high speed, high sensitivity electronics have been developed at USU that allow <10 nA, <5 μs pulsed beam measurements for determining insulator emission with minimal charging effects [17,23]. Optically isolated fast

(1-2 μs rise time) sensitive/low noise (10^7 V/A / 100 pA noise level) ammeters have been built to measure electron emission bursts that are emitted from the sample and detecting surfaces [17,23]. Detected current pulses from the ammeters are then either converted to total charge using integrator circuits, or sent to a fast digital storage oscilloscope and then exported to a computer for further analysis. A custom low-energy electron flood gun (energies <1 eV) is used to neutralize positive surface charging between pulses [17,23,25]; UV/VIS light sources are also available for charge neutralization [17]. Both DC and pulsed measurements and data retrieval are fully computer automated, using GPIB interfacing and a DAQ card under Labview™ control. Other detectors in the Fatman chamber include a standard Faraday cup detector, an electrostatic hemispherical analyzer, a cylindrical mirror analyzer, and a time of flight micro-channel plate detector. A complete description of the DC-system setup, as well as the pulsed-system setup, along with additional insulator-yield and charging data is available in other works [14,17,21,23].

Little boy chamber for energy- and angle-resolved emission studies

The USU facility is also equipped with a second, smaller UHV chamber, shown in Fig. 1, dedicated primarily to angle-resolved SE emission measurements [10,11,14,16]. The Little Boy chamber provides a highly controlled environment for low current measurements. A custom retarding field analyzer Faraday cup detector [10,11,13], continuously rotatable about the sample, is used to obtain angle-resolved SE yield and spectra for both normally and obliquely incident electrons in the range of emission angles $-16° < \alpha < +76°$ [10]. Angular resolution of the instrument is ~1.5° and the energy resolution is 0.2 eV ± 0.1% of the incident beam energy [10]. The chamber is equipped with a 0.3-3 keV electron source and a 100-500 eV ion source. In addition to angle-resolved measurements, this chamber has been used to study the dynamic evolution of SE yields as a function of surface condition [10-12] and sample potential [13].

Charge storage resistivity chamber

A third high vacuum chamber is available for insulator conductivity measurements using the charge storage method [20]. This chamber (see Fig. 1) is a second-generation system designed so that up to 32 samples on a rotatable carousel can be tested simultaneously in a controlled, stable vacuum environment for the duration of month-long experiments. Charge is deposited separately on each sample using a custom electron flood gun. [17,23]. The charge on the each sample is measured using the TreK™ charge probe [27] via a novel retractable charge transfer probe. These charge storage measurements are compared with thin film insulator conductivity measurements made using classical ASTM capacitor methods in a smaller vacuum vessel [18,28]. Both conductivity chambers allow temperature control over a range of approximately – 100 °C to + 100 °C, and controlled humidity, vacuum and ambient gas. Instrumentation for both classical and charge storage decay methods has been developed and tested in a joint project with the Jet Propulsion Laboratory (JPL) and USU. Details of the apparatus, test methods and data analysis and preliminary results are given elsewhere [18,19].

Capabilities at USU

The NASCAP code designed to model spacecraft charging uses 19 parameters to characterize the electronic properties of a given material [5]. Table I identifies the experimental methods and apparatus employed at USU to determine these 19 physical properties for each sample. The measurements can be grouped under three headings:

(i) sample characterization, used to fully identify the specific materials tested and to allow end users to more accurately assess which material is most closely related to their specific spacecraft materials;
(ii) electron emission (induced by electrons, ions, photons) which determine a material's response to space environment fluxes; and
(iii) conduction related properties, used to model the response of materials to accumulated charge.

The measurement methods and instrumentation are described below in more detail for each of these three groups. A number of additional property measurements, highlighted in italics in column three of Table I, are included in the study; the intent of these additional measurements is to extend the description of the electronic properties of the materials with the goal of improving the modeling of spacecraft charging in future codes. Further details of the instrumentation used for these measurements are found elsewhere [12,14].

Sample preparation and characterization

Conducting 1 cm diameter sample disks are polished using 0.25 μm diamond. Thin film samples are glued to a Cu slug using a UHV-adhesive and silver powder and the surface is cleaned by using standard solvents immediately prior to introduction into the vacuum. Surface morphology is characterized *ex situ* using optical microscopy, scanning electron microscopy subsequently mounted on a sample carousel in a UHV chamber (base pressure 10^{-9} to 10^{-10} Torr). *In situ* characterization of surface morphology is made with SEM. Auger electron spectroscopy (AES) mapping before and after electron emission measurements determined surface contaminants to a level of ~10% of a monolayer. Prior to taking yield measurements, many samples were ion sputtered with 500 eV argon ions at a typical fluence of ~5 $mC \cdot cm^{-2}$ to remove adsorbed contamination monolayers. Additional sample characterization capabilities are also available, including: photoelectron spectroscopy, and secondary ion mass spectroscopy for contamination assessment and IR/VIS/UVA reflectivity.

Electron-induced emission measurements

A primary focus of the research at USU has been the development of instrumentation and methods for measuring *absolute* total, SE, and BSE yields of conductor and insulator materials to incorporate into materials databases [24]. Emitted electrons can be divided into two categories: (i) Secondary electrons (SE): lower energy electrons (<50 eV by definition) that originate within the material, produced by numerous inelastic scattering events of the incident electrons, (ii) Backscattered electrons (BSE): typically higher energy electrons (>50 eV by definition) that originate from the incident electron source, but may scatter either elastically or inelastically before leaving the target material. The electron yields are then defined as the ratio of the sample emitted electron current captured by the detector to the total incoming electron current.

Table I. Methods and apparatus used for properties measurements related to NASCAP fit parameters.

Property Category	Measured Property (Methods and Apparatus)	Related NASCAP Parameters [5, *]
Sample Character-ization	Density (Gravimetric)	Density; ρ {9,19}.
	Bulk Composition (AA, ICP)	Mean atomic number <Z> {4} and weight <A> {10}.
	Surface contamination (*in situ* AES, AES mapping)	
	Surface morphology *(in situ* SEM.; *ex situ* STM/AFM, SEM, optical microscopy)	
	Coating thickness *(in situ* HEED; *ex situ* STM/AFM, SEM, optical microscopy)	Dielectric film thickness; d {2}.
Conduction Related Properties	Dielectric constant *(ex situ* capacitive measurements)	Relative dielectric constant; ε_r {1}.
	Bulk and surface conductivity (*ex situ* 4-point resistance probe measurements, ASTM capacitance resistance, charge storage decay)	Bulk conductivity; σ_o {3}. Surface resistivity; ρ_s {14}. *Temperature dependence of conductivity. Charge storage resistivity.*
	Electrostatic discharge *(in situ* I-V profiles of non-conducting films on conducting substrates)	Maximum potential before discharge to space; V_{max} {15}. Maximum surface potential difference before dielectric breakdown discharge; V_{punch} {16}.
	High-energy plasma radiation-induced conductivity (IV measurements for flux of monoenergetic electrons for non-conductive samples)	Two parameter fit of radiation-induced conductivity, σ_r; k and Δ {17, 18}.
Electron-Induced Emission	SE/BES total yields versus incident electron energy (Emission current for flux of monoenergetic electrons from 100 eV to 30 keV).	Maximum SE yield δ_{max} {5}. Energy for δ_{max}; E_{max} {6}. Effective atomic number, Z_{eff}, for $\eta(E_o)$ {4}. *Extended parameter fits for $\delta(E_o)$ and $\eta(E_o)$. Incident angle dependence of $\delta(E_o)$ and $\eta(E_o)$*
	Stopping power data.	Four-parameter bi-exponential range law fit for PE energy range derived from stopping power data; b_1, n_1, b_2, n_2 {7-10}.
	Energy- and angle- resolved BS/SE cross sections. (Cross sections using rotatable Faraday cup retarding field analyzer.)	*Parameters for Lambert cosine law fit of angular-resolved cross sections* [13]. *Parameters for Chung and Everhart* [26] *model of energy- resolved cross section. Parameters for coupled energy-angle resolved cross section* [12,13].
Ion-induced Emission	Total electron yield versus incident ion energy (Emission current from flux of monenergetic He ions at 100 eV to 5 keV)	SE yield due to 1 keV proton impact; δ^H(1keV) {11}. Incident proton energy for δ^H_{max}; E^H_{max} {12}. *Ion energy dependence of emitted electron yields. Energy spectra of emitted electrons. Species dependence of ion yields.*
Photon-induced Emission	Total electron yield versus incident photon energy (Emission current for flux of monoenergetic photons from discharge lamps)	Total electron yield from solar spectrum {13}. *Photon energy dependence of emitted electron yields. Energy spectra of emitted electrons.*

* The numbers of the materials database parameters used in the current version of NASCAP are indicated in curly brackets. Proposed additions to the database are indicated in italics.

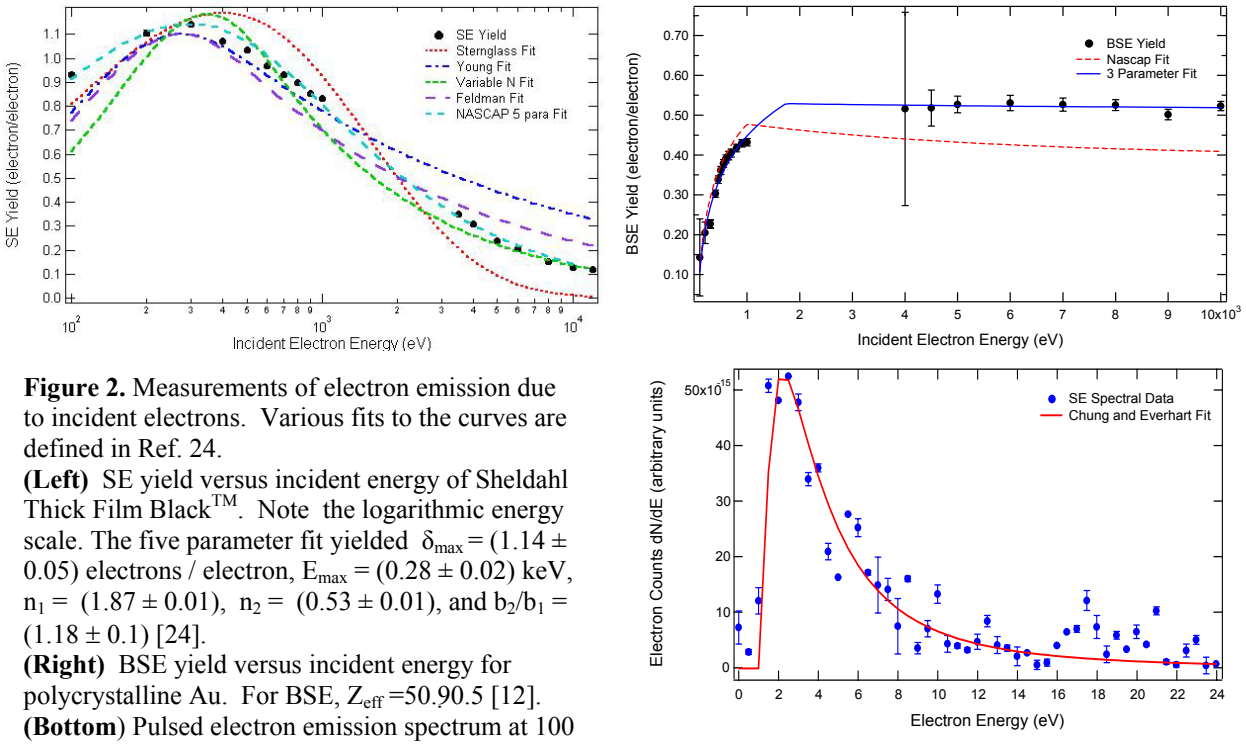

Figure 2. Measurements of electron emission due to incident electrons. Various fits to the curves are defined in Ref. 24.
(Left) SE yield versus incident energy of Sheldahl Thick Film Black™. Note the logarithmic energy scale. The five parameter fit yielded $\delta_{max} = (1.14 \pm 0.05)$ electrons / electron, $E_{max} = (0.28 \pm 0.02)$ keV, $n_1 = (1.87 \pm 0.01)$, $n_2 = (0.53 \pm 0.01)$, and $b_2/b_1 = (1.18 \pm 0.1)$ [24].
(Right) BSE yield versus incident energy for polycrystalline Au. For BSE, $Z_{eff} = 50.90.5$ [12].
(Bottom) Pulsed electron emission spectrum at 100 eV incident energy for Ti alloy. [22]

Figure 2 shows the total, SE, and BSE yields as functions of normal incident electron energy over a range of ~<100 eV to 10 keV using the DC-yield apparatus and also the energy-resolved emission spectra using the pulsed-yield apparatus. Such measurements on conductors are straightforward, since a constant electron current source can be used and DC currents from the sample can be captured and quantified using the detector assembly and a sensitive slow-response picoammeter. Additionally, by grounding the conductor, any charge that leaves or is absorbed into the material can be immediately neutralized to ground. Electron yield measurements on dielectrics are more difficult to make than on conductors, since any charge that is deposited in the material cannot easily be dissipated. The surface and bulk potentials that develop can subsequently affect electron emissions by either influencing incident electron energies, or by creating internal electric fields that alter the escape mechanisms of SE's. Consequently, for insulators the pulsed-yield apparatus with neutralization methods must be used.

In order to predict the extent of spacecraft differential charging in modeling codes it is mandatory to accurately determine *absolute* SE yield parameters that include the maximum electron yield, δ_{max} and its corresponding energy, E_{max} as well as the first and second crossover energies, E_1 and E_2, at which the material transitions between positive and negative charging. The two parameters δ_{max} and E_{max} are used in NASCAP to model the SE yield as a function of incident energy. Four additional parameters, b_1, n_1, b_2, n_2, are used to describe the shape of the reduced yield curve $\delta(E_0)/\delta_{max}$ vs. E_o/E_{max} . They are typically determined from a bi-exponential range law fit for PE energy range derived from stopping power data [5]. They can also be determined directly from fits to the SE yield curve; in this case b_2 and n_2 describe the shape of the high energy tail of the curve while b_1 and n_1 model the region from E_{max} to a few keV incident energies [12,28]. In addition, we determined alternate fits to the reduced yield curve using a number of other models which potentially provide more accurate models, particularly in

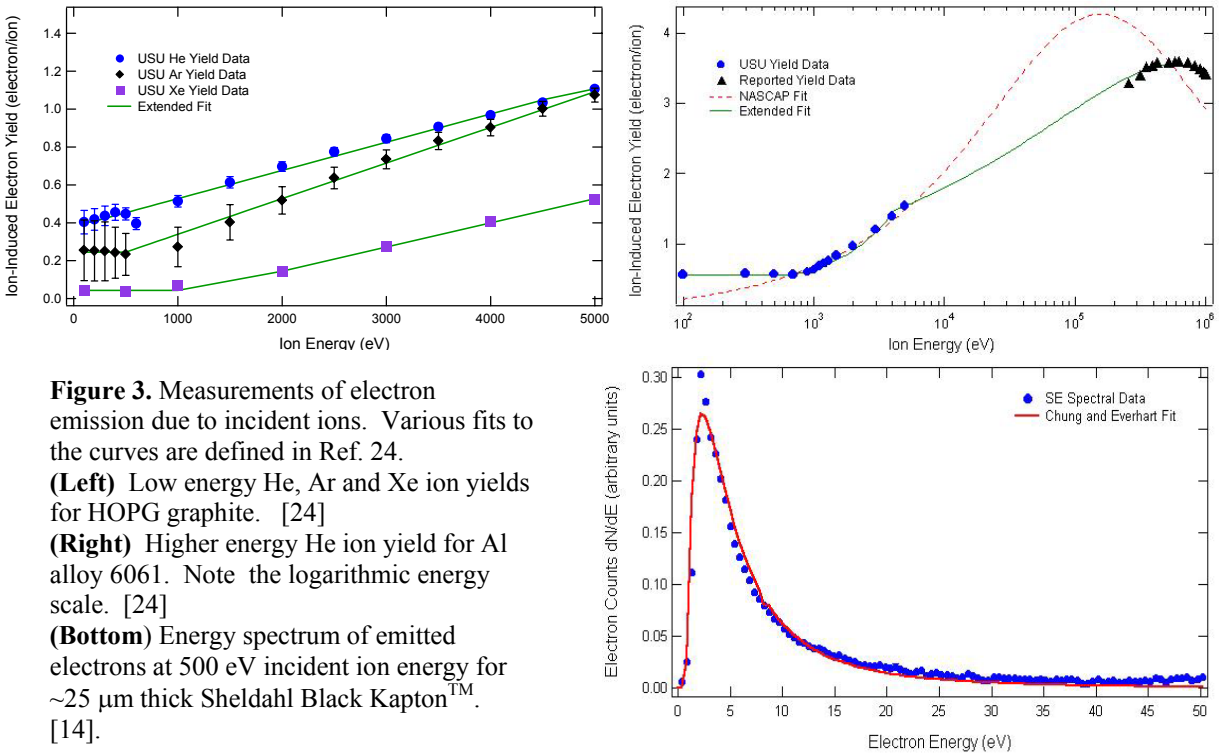

Figure 3. Measurements of electron emission due to incident ions. Various fits to the curves are defined in Ref. 24.
(Left) Low energy He, Ar and Xe ion yields for HOPG graphite. [24]
(Right) Higher energy He ion yield for Al alloy 6061. Note the logarithmic energy scale. [24]
(Bottom) Energy spectrum of emitted electrons at 500 eV incident ion energy for ~25 μm thick Sheldahl Black Kapton™. [14].

the high energy tail, including those by Sternglass [29], Schwartz [30], and Dionne [31]. The BSE yield curve is modeled in NASCAP using a very complex function with a single parameter, the effective atomic number, Z_{eff} [5]. Note that Z_{eff} is not related to the atomic number of the sample. This and a more elaborate empirical five parameter fit are shown in Fig. 2. A four-parameter fit, based on the work of Chung and Everhart [26], is used to model the emission spectra (see Fig. 2). Other measurement and analysis methods are being explored to determine insulator yield parameters free from charging distortions. For example, three approaches have been used at USU successfully to determine the second crossover energy, E_2 for insulating materials: (i) the mirroring method approach; (ii) the pulsed-total yield approach; and (iii) and the dc-spectral approach [22]. Of these two techniques, the dc-spectra approach is found to be most sensitive to sample negative charging, and therefore a more precise method for determining E_2.

Ion-induced emission measurements

Total electron yield due to ion bombardment as a function of incident ion energy and emission spectra (see Fig. 3) are measured using the same hemispherical grid retarding field analyzer used for SE/BSE emission measurements. A cold cathode ion gun is used as the source for monoenergetic He, Ne, Ar, Kr and Xe ions over the range of <100 eV to 5000 eV. The sample is biased to -20 eV to repel SE which would contaminate the emission measurements.

NASCAP requires two ion yield fitting parameters: (i) the SE yield due to 1 keV proton impact,. δ^H_{1keV}, and (ii) the incident proton energy, E^H_{max},for maximum ion yield, δ^H_{max} [5]. Our measurements do not go to high enough energies to determine E^H_{max}, which is typically 100 keV or higher; therefore, high energy yields from the literature are used to augment the USU low energy data. Figure 3 shows both the NASCAP fit and an extended 5 parameter empirical fit, plus the ion yield dependence on ion mass [14,24]. Our lowest mass measurements were done

with He rather than incident protons; however, this does not present a significant problem as the difference between H and He yields is typically not large, where data are available, and further NASCAP assumes that the emission is the same for all ion species, independent of mass [5].

Photon-induced emission measurements

Total electron yields due to photon bombardment as a function of incident photon energy (see Fig. 4) are determined by measuring incident beam and sample currents. The sample is biased to -20 eV to repel SE which would contaminate the emission measurements. NASCAP uses a single parameter, the total electron yield due to standard solar irradiance, to characterize photon-induced electron emission [5]. It is straightforward to determine this parameter from integration of the measured spectra of electron emission versus incident photon energy (see Fig. 4), by normalizing for the solar spectral intensity [32].

Conduction related properties

Conductivity of insulating materials is a key parameter to determine how accumulated charge will distribute across the spacecraft and how rapidly charge imbalance will dissipate. Instrumentation for both classical and charge storage decay resistivity methods has been developed and tested at JPL and USU. Details of the apparatus, test methods and data analysis are given elsewhere [18-20]. Classical methods use a parallel plate capacitor configuration to determine the conductivity of insulators by application of a constant voltage (E field) and the measurement of the resulting leakage current across the plates and through the insulator [18,28]. The capacitive resistance apparatus (CRA) at USU is designed as a versatile instrument for classical resistance measurements under tightly controlled conditions [18]. The sample environment—including sample temperature, ambient vacuum or background gas, and humidity—can be strictly controlled. Computer automation of voltage and current measurements, together with environmental parameters, allow rapid and prolonged resistance measurements. Thus, the apparatus is capable of parametric studies of variables that influence the resistivity, including sample material and thickness, applied voltage magnitude and duration, sample temperature, ambient gas or vacuum, and humidity. Figure 5 shows data obtained at USU using the classical resistance method following the ASTM D 257-99 standard method [28] for Sheldahl [33] thermal control blanket material at 26±2 °C in ambient room light at 30±5% ambient relative humidity with wet electrodes for a range of voltages. The curves showed linear behavior on a log-log plot with a slope of ~½ and converged to ~$(3\pm1)\cdot10^{+16}$ Ω·cm at ~½ hr. The published resistivity value for Dupont Kapton HN is $1\cdot10^{17}$ Ω·cm [34].

However, recent works have shown that these classical methods are often not applicable to situations encountered in spacecraft charging [18,20,35]. Conductivity is more appropriately measured for spacecraft charging applications as the "decay" of charge deposited on the surface of an insulator. Charge decay methods expose one side of the insulator in vacuum to sequences of charged particles, light, and plasma, with a metal electrode attached to the other side of the insulator. Data are obtained by capacitive coupling to measure both the resulting voltage on the open surface and emission of electrons from the exposed surface, as well monitoring currents to the electrode.

Additional equipment is available for *ex situ* examination of conduction-related properties, including capacitance, bulk and surface conductivity, dielectric constant, dielectric strength and electrostatic discharge [24]. The relative dielectric constant and bulk resistivity were measured

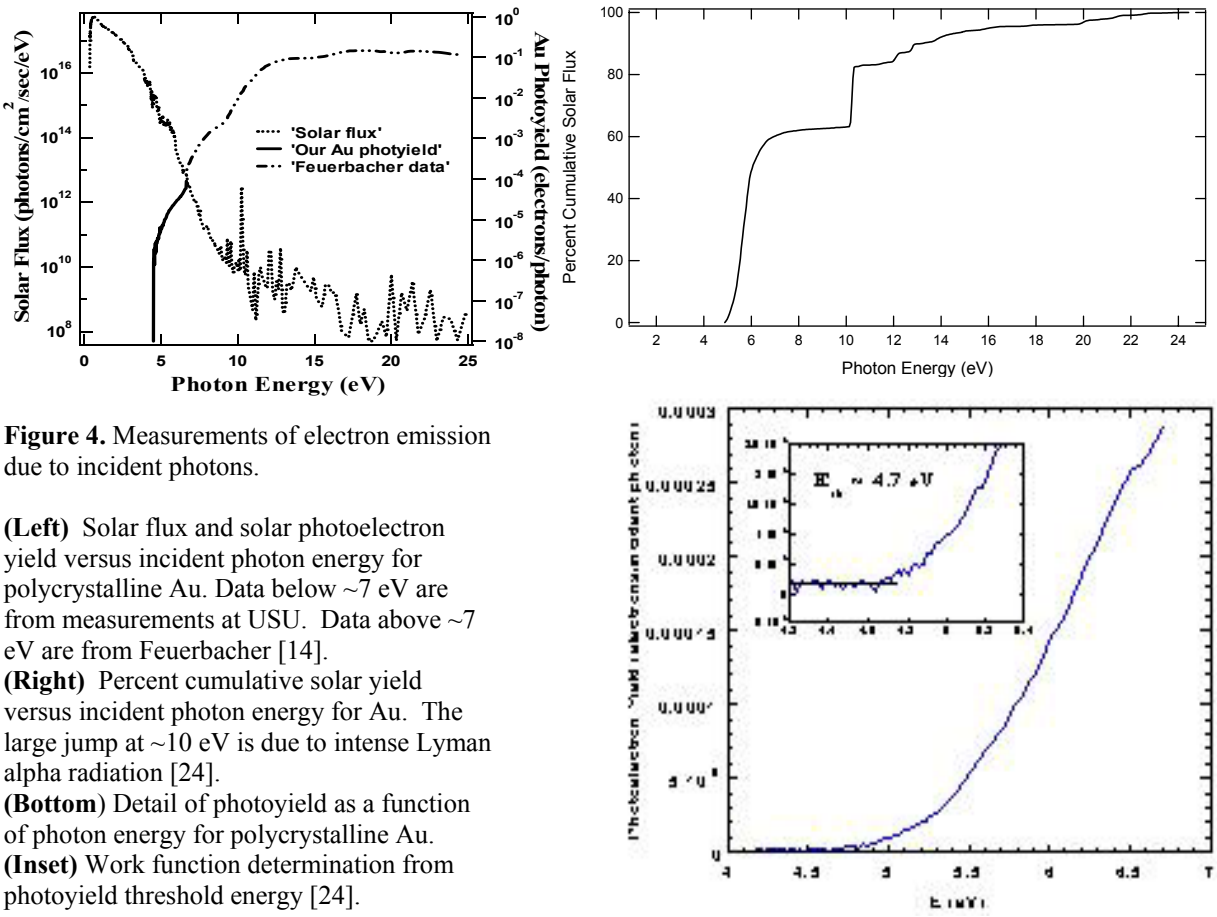

Figure 4. Measurements of electron emission due to incident photons.

(Left) Solar flux and solar photoelectron yield versus incident photon energy for polycrystalline Au. Data below ~7 eV are from measurements at USU. Data above ~7 eV are from Feuerbacher [14].
(Right) Percent cumulative solar yield versus incident photon energy for Au. The large jump at ~10 eV is due to intense Lyman alpha radiation [24].
(Bottom) Detail of photoyield as a function of photon energy for polycrystalline Au.
(Inset) Work function determination from photoyield threshold energy [24].

using a standard impedance analyzer (see Fig. 5). A standard four-point probe is used for *ex situ* measurements of bulk and surface conductivity of more conducting samples. The maximum potential difference that can exist between the material surface and the underlying conductor before dielectric breakdown or "punchthrough" is referred to as the punchthrough voltage or dielectric strength. The punchthrough voltage of thin insulating films was measured using the Utah State custom capacitor resistance apparatus by monitoring current across the sample while applying voltage across the sample electrodes. Alternatively, dielectric breakdown can be determined by high energy bombardment. Above 1600 eV incident electron beam energy, the anodized Al surface layer reached its breakdown potential and became conducting, passing DC-current through the sample as shown in Fig. 5.

Application to Spacecraft Charging

The primary object for the SEE projects at USU was to provide an extensive database of electronic properties of relevant spacecraft materials for use in charging codes. Table II lists values of the 19 parameters used to specify materials properties in NASCAP for a representative sample, Au. Our studies are posted on the web-browser based *Database of Electronic Properties of Materials Applicable to Spacecraft Charging* in the *SEE Charge Collector Knowledgebase* [36]. This *Database* contains a *Materials Report* for each sample studied which has a detailed description of the source of the sample, all measured characterization data, the raw emission data, the derived values for NASCAP parameters and other models of the data, and a review of the available literature on the material [24]. The parameters for NASCAP derived from a

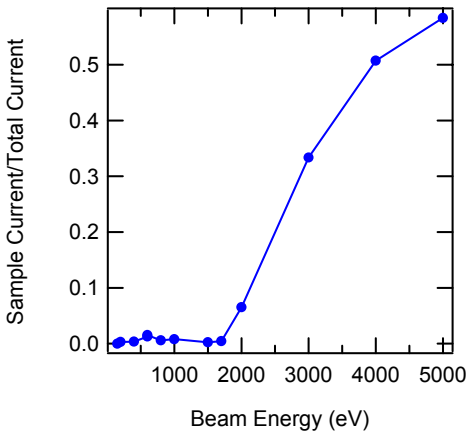

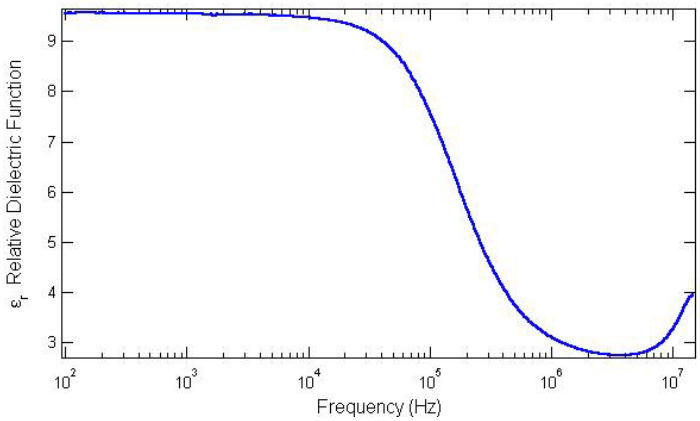

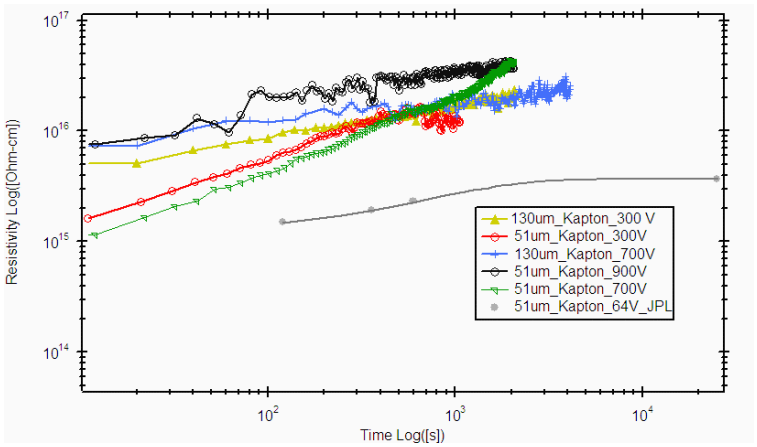

Figure 5.Conduction related properties **(Top)** Relative dielectric constant versus frequency for 25 µm Kapton HN film with ~0.1 µm vapor-deposited Al and ~40 nm indium tin oxide (ITO) coatings. The sample was a composite material sold for applications as a low emissivity conductive thermal control coating material for spacecraft [33,34]. **(Bottom)** Classical resistivity versus time measurements for a sample of Sheldahl thermal control blanket material with a Kapton HN substrate and a 0.1 µm vapor-deposited Al coating [33,34]. Data shown are from USU for 51 µm and 130 µm thick samples at 300 V, 700 V and 900 V uncoated sample at 64 V [22]. JPL data are for 51 µm thick uncoated sample at 64 V [19]. **(Bottom)** Discharge current versus electron beam incident energy for 1 µm thick chromic acid anodized Al 2219 alloy. Breakdown initiates at ~1600 eV incident energy, at the sample current threshold [22].

representative Au data set are listed in Table III. Additional analysis and parameterization for improved material modeling in future spacecraft charging codes (see below) is also included in each *Materials Report*.

Table III is a list of the materials already on reported in the *Database* and those currently being tested at USU. The prioritized list is based on extensive discussions with spacecraft charging community specialists, intended to meet two objectives: (i) extending the NASCAP database to include the most common spacecraft materials currently in use and (ii) investigating representative materials with wide ranging physical properties. The accurate remeasurement of NASCAP parameters for those materials already incorporated in current NASCAP databases serves to confirm our experimental methods or update existing data which are not fully reliable.

Suggested improvements to materials properties parameterization

Based on our experience with materials testing and characterization, data analysis, and evaluation of spacecraft charging, we can offer recommendations for additional measurements and improved parameterization of existing results that can be used to improve the modeling of spacecraft charging in future codes. Specifically, we suggest:

i) *Extended Parameterization*: Enhance modeling of electron emission data with extended parameter fits. Specifically, add a 6 parameter empirical BSE yield fit and a 5 parameter empirical ion yield fit.

ii) *Additional Emission and Optical Properties:* Extend modeling to include electron emission spectra, work functions, and angular distribution of emitted electrons to more fully model the effects of surface bias on yields and return currents. Add ion species (mass) dependence to ion yield models. Extend photoyield models to include photon energy dependant yields; this can model varying incident optical spectra and reflected or partially transmitted light. Incorporate reflectivity spectra to model fraction of incident light causing photoemission and indirect photoemission.

iii) *Data Modeling:* Add capabilities within NASCAP to fit data sets of new materials using the NASCAP parameterized models, especially the 5 parameter SE yield model.

Table II. Spacecraft Materials Tested at Utah State University.

Conducting Materials

Elemental Metals and Semiconductors	Alloys	Conductive Coatings
Aluminum (Al)	Al Alloy 6061-T6	Aquadag (C)
Beryllium (Be)	Stainless Steel Alloy 316	Amorphous Carbon (a-C)
Copper (Cu)	Ti Alloy Ti-A16-v4	
Gold (Au)		Annealed Amorphous Carbon
HOPG Graphite (C)		
Molybdenum (Mo)		
Silver (Ag)		

Spacecraft Materials

Conductors	Insulators
Carbon-filled polyester (Sheldahl Thick Film Black)	Ge on 25 µm Kapton (Sheldahl thermal control blanket)
Black Kapton conducting (Sheldahl thermal control blanket)	ITO on 50 µm FEP with Ag/Inconnel backing (Sheldahl thermal control blanket)
	ITO on 25 µm Kapton with Al Backing (Sheldahl thermal control blanket)
	8 µm Kapton on Al backing (Sheldahl thermal control blanket)
	6.4 µm PET on Al backing (Sheldahl thermal control blanket)
	13 µm FEP on Ag/Inconnel backing (Sheldahl thermal control blanket)
Conductive Coatings	**Non-Conductive Coatings**
Al on 2 µm Kapton (JPL "Solar Sail")	RTV Adhesive (DC 93-500) on Cu
Al on 8 µm Kapton (Sheldahl thermal control blanket)	RTV Adhesive (CV-1147) on Cu
Al on 25 µm Kapton with ITO backing (Sheldahl thermal control blanket)	Anodized (Cr-Acid) Al Alloy
Al on 6.4 µm PET (Sheldahl thermal control blanket)	Anodized (S-Acid) Al Alloy
Ag/Inconel on 13 µm FEP (Sheldahl thermal control blanket)	

SEE Materials Database (Ver. 2) materials in green.
Materials currently under study at USU in red.

iv) *Charge Transport Capabilities:* Add charge storage method resistivity values to the database [24]. Add parametric models of resistivity (*e.g.,* temperature or electric field dependence) and dielectric spectra useful in charge transport modeling. Expand modeling of radiation-induced conductivity and electron emission based on the internal charge distribution of insulators [22].

v) *Multi-Material Geometries:* Enhance multi-material geometry capabilities to better model semi-transparent (to electrons, ions or light) thin-film conductors/insulators on conducting/insulating substrates. This capability will be essential to more fully model contamination and surface modification, in addition to optical, thermal and atomic oxygen resistant coatings [12,13].

Other Applications

In addition to direct contributions to the *Database of Electronic Properties of Materials,* there have been a number of studies at USU on specific aspects of the contributions of electron emission to the overall spacecraft charging problem. One such study has determined that, under certain circumstances encountered in near-earth orbits, incorporating more complete knowledge of the energy- and angle-resolved spectra of SE is necessary to fully model how SE emission and spacecraft charging are affected by re-adsorption of low energy electrons by the emitting surface or adjacent surfaces in the presence of charge-induced electrostatic fields [13]. Angular distribution of SE's were found to affect charging calculations when a spacecraft is charged positively and can also affect return current to adjacent surfaces [13]. Angle- and energy-resolved spectra $\eta(E,\alpha)$ and $\delta(E,\alpha)$ were measured for selected conducting materials [11,16], and these data were used to quantitatively model the effects of sample bias and the interplay between spacecraft geometry and angular emission.

These same angle- and energy-resolved emission spectra have also been compared to theoretical predictions of the emission cross sections. Semi-empirical theory assumes isotropic angular distribution, [37] while quantum theory predicts highly anisotropic angular production cross sections that become isotropic during transport to the surface [38]. Our studies indicate that there may still be anisotropic components to some energy ranges as vestiges of the underlying SE production mechanisms [11,16].

We have also studied the effects of bandgap and surface potential barriers on emission from semiconductors and insulators [21,23,39]. One study shows that $_{,max}$ decreases by ~30% as the bandgap of graphitic amorphous carbon decreases from ~0.6 to ~0 eV upon thermal annealing [21,39]. Other studies look at the role of band gap and electron affinity on emission from insulators [23]. In this and other studies, we attempt to understand how the fundamental physics mechanisms and the interaction of electrons with matter underlying three phase models of the production, transport and emission from a surface are related to the observed emission [16,21,23].

Emission of low energy SE is very surface sensitive. Therefore, even monolayer contamination can significantly modify SE yield. USU studies of deposition of disordered carbon on Al/Al_2O_3 and Au surfaces found that modification of only a couple atomic layers led to changes in SE yields by a factor of 2 or more; further modeling of hypothetical satellites suggested monolayer C contamination of Au can swing charging 10^4 V! [10,12]

We have also studied the contribution to "snapover" from SE emission [40,41]. In snapover, insulators surrounded by positively biased conductors in a plasma experience a surface discharge phenomena. Our studies suggest that secondary emission is not the only factor that determines the onset positive voltage for snapover [23].

Spin-off application

While the primary motivation for our work at USU is based on charging of spacecraft materials [14,24], the electron emission properties of materials are relevant to many spin-off technical applications. Electron multipliers use high SE yield dynode materials [42]. Material and topographic contrast in scanning electron microscopy exploit the facts that the number of SE's produced depends on the electronic structure and angular distribution of emitted electrons, respectively [37,43]. Electron probe microanalysis and Auger electron spectroscopy are surface techniques based on details of backscattered electron energy loss mechanisms [44]. SE yield from emitters is critical in design of field emission devices [45]. Electron emission has important applications for next generation flat panel displays; electron emission sources must have high yields and the spacers between anodes and cathodes are required to be insulating and have low SE yields [46]. Advanced vacuum tube technology requires low SE yield materials [47]. SE yield of materials determines arc initiation, with important applications to high power arcing [48] and plasma discharge phenomena like flashover or snapover [40,41]. Disordered carbon is used to coat the inside of the plasma fusion confinement test reactors to reduce secondary electron emission that inhibits controlled fusion reactions [49].

Table III. NASCAP parameters for polycrystalline Au [14].

Parameter	Value
[1] Relative dielectric constant; ε_r (Input as 1 for conductors)	1, NA
[2] Dielectric film thickness; d	0 m, NA
[3] Bulk conductivity; σ_o (Input as -1 for conductors)	$(3\pm1)\cdot10^{7}\Omega^{-1}\cdot m^{-1}$
[4] Mean atomic number $<Z_{eff}>$	50.9±0.5
[5] Maximum SE yield for electron impact; δ_{max}	1.47±0.01
[6] Primary electron energy for δ_{max}; E_{max}	(0.57±0.07) keV
[7-10] Fit to stopping power data; b_1, n_1, b_2, n_2	n_2=1.39±0.04 b_2=1, n_1=0, b_1=0
[9 and 19] Density; ρ	$(1.932\pm0.002)\cdot10^{4}$ kg·m^{-3}
[10] Mean atomic weight <A>	196.97
[11] SE yield due to proton impact δ^{H}(1keV)	(0.336±0.002) .
[12] Incident proton energy for δ^{H}_{max}; E^{H}_{max}	(1238±30) keV
[13] Photoelectron yield, normally incident sunlight	$3.64\cdot10^{-5}$A·m^{-2}
[14] Surface resistivity; ρ_s	-1 ohm, NA
[15] Max. potential before discharge to space; V_{max}	10000 V, NA
[16] Maximum surface potential difference before dielectric breakdown discharge; V_{punch}	2000 V, NA
[17, 18] Two parameter fit of radiation-induced conductivity, σ_r; k and Δ	NA

NA -- Not applicable or approximated for bulk conductors.

Acknowledgments

The research described here was primarily supported through a contract with the NASA Space Environment and Effects (SEE) Program [15]. Instrumentation was funded primarily from the AFOSR (DURIP) Program and the USU Research Office. Additional funding was provided by Boeing, Thiokol, and Advanced Scientific. Funding for students was provided by the NASA SEE Program, NASA Graduate Student Researcher's Program, NASA Rocky Mountain Space Grant Consortium, USU Space Dynamics Laboratory, and USU Research Office URCO grants.

References

1. R.D. Leach, and M.B. Alexander: "Failures and Anomalies Attributed to Spacecraft Charging," NASA Reference Publication 1354, NASA Marshall Space Flight Center, November 1994.

2. D. Hastings, and H. Garrett, Spacecraft-environment Interactions, Cambridge University Press, 1996.

3. K.L. Bedingfield, R.D. Leach and M.B. Alexander,: "Spacecraft System Failures and Anomalies Attributed to the Natural Space Environment." NASA Reference Publication 1390, NASA MSFC, 1996.

4. M.R. Carruth Jr., T. Schneider, M. McCollum, M. Finckenor, R. Suggs, D. Ferguson, I. Katz, R. Mikatarian, J. Alred, and C. Pankop, "ISS and space environment interactions without operating plasma contactor," AIAA Paper #2001-0401, Proc. of the 39th AIAA Aerospace Sci. Meeting, Reno, Nevada, Jan. 8-11, 2001.

5. M.J. Mandell, P.R. Stannard and I. Katz, "NASCAP Programmer's Reference Manual," NASA LRC, 1993.

6. Myron Mandell, "NASCAP-2K – An Overview"," Proc. of 8th Spacecraft Charging Techn. Conf., October 20-24, 2003, Huntsville, Alabama.

7. Marc Van Eesbeek, Alain Hilgers, "European Approach to Materials Characterization for Plasma Interactions Analysis," Proc. of 8th Spacecraft Charging Techn. Conf.,, October 20-24, 2003, Huntsville, Alabama.

8. V.A. Davis, L.F. Neergaard, M.J. Mandell, I Katz, B.M. Gardner, J.M. Hilton, J. Minor, "Spacecraft Charging Calculations: NASCAP-2K and SEE Spacecraft Charging Handbook," AIAA 2002-0626, Proc. 40th AIAA Aerospace Sci. Meeting, January 14-17, 2002, Reno, Nevada.

9. Sebastien Clerc, S. Brosse, M. Chane-Yook, SPARCS: An Advanced Software For Spacecraft Charging Analysse," Proc. of 8th Spacecraft Charging Techn. Conf., October 20-24, 2003, Huntsville, Alabama.

10. R.E. Davies and J.R. Dennison, J. Spacecraft and Rockets, 34, 571-574 (1997).

11. R.E. Davies, "Backscattered and Secondary Electron Scattering Measurements with Applications to Spacecraft Charging," MS Thesis, Utah State Univ., 1996.

12. W.Y. Chang, J.R. Dennison, Jason Kite and R.E. Davies, "Effects of Evolving Surface Contamination on Spacecraft Charging," Proc. of the 38th AIAA Aerospace Sci. Meeting, Reno, NV, January 12, 2000.

13. N. Nickles, R.E. Davies and J.R. Dennison, "Applications of SE Energy- and Angular-Distributions to Spacecraft Charging," Proc. of 6th Spacecraft Charging Techno. Conf., (Hanscom Air Force Base, MA, 1999).

14. W.Y. Chang, J.R. Dennison, Neal Nickles and R.E. Davies, "Utah State University Ground-based Test Facility for Study of Electronic Properties of Spacecraft Materials," Proc. of 6th Spacecraft Charging Techno. Conf., (Hanscom Air Force Base, MA, 1999).

15. JR Dennison, NASA Space Environments and Effects Program Grants, "Electronic Properties of Materials with Application to Spacecraft Charging," 1998-2003; "Electronic Properties of Materials with Application to Spacecraft Charging—Extension of Materials Database," 2003-2004.

16. R.E. Davies, "Measurement of Angle-Resolved SE Spectra," PhD Thesis, Utah State Univ., 1999.

17. C.D. Thomson, V. Zavyalov, J.R. Dennison, "Instrumentation for studies of electron emission and charging from insulators," Proc. of 8th Spacecraft Charging Techn. Conf.,, October 20-24, 2003, Huntsville, Alabama.

18. Prasanna Swaminathan, A. R. Frederickson, J.R. Dennison, Alec Sim, Jerilyn Brunson, Eric Crapo, "Comparison Of Classical And Charge Storage Methods For Determining Conductivity Of Thin Film Insulators," Proc. of 8th Spacecraft Charging Techn. Conf., October 20-24, 2003, Huntsville, Alabama.

19. J.R. Dennison, A. R. Frederickson, Prasanna Swaminathan, "Charge Storage, Conductivity And Charge Profiles Of Insulators As Related To Spacecraft Charging," Proc. of 8th Spacecraft Charging Techn. Conf., October 20-24, 2003, Huntsville, Alabama.

20. A.R. Frederickson and J.R. Dennison, "Measurement of Conductivity and Charge Storage in Insulators Related to Spacecraft Charging," Proc. 2003 IEEE Nuclear and Space Radiation Effects Conference, Monterey, CA, July 21-25, 2003; to be published in IEEE Transaction on Dielectrics and Electrical Insulation.

21. Neal Nickles, "The Role of Bandgap in the SE Emission of Small Bandgap Semiconductors: Studies of Graphitic Carbon," PhD Dissertation, Utah State Univ., August 2002.

22. C.D. Thomson, V. Zavyalov, J.R. Dennison, Jodie Corbridge, "Electron Emission Properties Of Insulator Materials Pertinent To The International Space Station," Proc. of 8th Spacecraft Charging Techn. Conf., October 20-24, 2003, Huntsville, Alabama.

23. C.D. Thomson, Measurements of the SE Emission Properties of Insulators, Ph.D. dis., Utah State Univ., 2004.

24. J.R. Dennison, W.Y. Chang, N. Nickles, J. Kite, C.D. Thomson, Jodie Corbridge, and Carl Ellsworth, "Final Report Part III: Materials Reports," NASA Space Environments and Effects Program Grant, "Electronic Properties of Materials with Application to Spacecraft Charging," September 2002; J.R. Dennison, J. Kite, C.D. Thomson, Jodie Corbridge, Robert Berry, and Carl Ellsworth, "Final Report Part IV: Additional Materials Reports," May 2003. Available in electronic format through NASA SEE as part of the SEE Charge Collector Knowledgebase, http://see.msfc.nasa.gov/ee/db_chargecollector.html.

25. I. Krainsky, W. Lundin, W.L. Gordon, and R.W. Hoffman, Secondary Electron Emission Yield Annual Report for Period July 1, 1979 to June 30, 1980, Case Western Reserve University, Cleveland, OH, 1980 (unpub.).

26. Chung, M.S. and T.E. Everhart, "Simple calculation of energy-distribution of low-energy SEs emitted from metals under electron bombardment," J. Appl. Phys. 45,2, 707-709, 1974.

27. Operators Manual, Model 341A, High Voltage Electrostatic Voltmeter, Trek, Inc., 11601 Maple Ridge Road, Medina, New York 14103, USA. Telephone: (585) 798-3140, http://www.trekinc.com/.

28. ASTM D 257-99, "Standard Test Methods for DC Resistance or Conductance of Insulating Materials" (American Society for Testing and Materials, 100 Barr Harbor drive, West Conshohocken, PA 19428, 1999).

29. Mandell, private communications, 2000.

30. Sternglass, E.J., "Theory of SE emission by high-speed ions," Phys. Rev. 108, 1, 1-12 (1957).

31. Schwarz, A., "Application of a semi-emperical sputtering model to secondary electron emission," J. Appl. Phys. 68 2382 (1990).

32. Gerald F. Dionne, "Origin of SE emission yield-curve parameters," J. Appl. Phys. 46 (8), 3347-3351 (1975).

33. B. Feuerbacher and B. Fitton, J. Appl. Phys. 41 1536 (1972).

34. The Red Book, RB 1, (Sheldahl Technical Materials, Northfield MN, 1995); http://www.sheldahl.com/Product/TechMaterials.htm, June 20, 2002.

35. Kapton polyimide film product information: Physical Properties, Report H-38492-1, (Dupont, Wilmington, DE, February, 1997); http://www.dupontteijinfilms.com/ , June 20, 2002.

36. A.R. Frederickson, C. E. Benson and J. F. Bockman, "Measurement of Charge Storage and Leakage in Polyimides," Nuclear Instruments and Methods in Physics Research B, 454-60, 2003.

37. NASA Space Environments and Effects Program SEE Charge Collector Knowledgebase, http://see.msfc.nasa.gov/ee/db_chargecollector.html.

38. L. Reimer, Scanning Electron Microscopy. Physics of Image Formation and Microanalysis, (Springer-Verlag., 1985), pp. 119-121.

39. M. Rösler and W. Brauer, "Theory of secondary electron emission I. General theory for nearly-free-electron metals," Phys. Stat. Sol. (b), 104, 161-175, 1981.

40. Jodie Corbridge and J.R. Dennison, "Effects of Bandgap on SE Emission for Graphitic Carbon Semiconductiors," Bull. Am. Phys. Soc. 48(1) Part II, 1146, (2003).

41. C.D Thomson, J.R Dennison, R.E Davies, B Vayner, J Galofaro, D.C Ferguson, and W. de Groot, "Investigation of the Snapover of Positively Biased Conductors in a Plasma," Proc. 38th AIAA Aerospace Sci. Meeting, January 10-13, 2000, Reno, Nevada.

42. C.D. Thomson, "Experimental Investigation of Snapover: The Sudden Increase of Plasma Current Drawn to a Positively Biased Conductor When Surrounded by a Dielectric," M.S. Thesis, Utah State University, 2001.

43. W. E Baumgartner, W. K Huber, "SE emission multipliers as particle detectors," J. Phys. E: Sci. Instrum., 9(5), 321-30 (1976).

44. H. Seiler, "SE emission in the scanning electron microscope," J. Appl. Phys. 54 (11), R1-R18 (1983).

45. H. Ibach, Electron Spectroscopy for Surface Analysis (Springer-Verlag, New York, 1977).

46. P. R Schwoebel, I. Brodie, "Surface-science aspects of vacuum microelectronics," J. Vacuum Sci. Techn., B, 13(4), 1391-410 (1995).

47. G. Auday, Ph. Guillot, and J. Galy, "Secondary emission of dielectrics used in plasma display panels," J. Appl. Phys. 88 (8), 4871-4874 (2000).

48. P. A Redhead, "The birth of electronics: Thermionic emission and vacuum," J. Vacuum Sci. Techn., A, 16(3, Pt. 1), 1394-1401 (1998).

49. G. R. Jones, M. T. C. Fang, "The physics of high-power arcs," Reports Prog. Phys., 43(12), 1415-65 (1980).

50. Kaoru Ohya, "SE emission from plasma facing materials and its impact on sheath voltage," Nuclear Instruments and Methods in Physics Research, Section B: Beam Interactions with Materials and Atoms (1999).